Journal of Molecular Histology
https://doi.org/10.1007/s10735-021-09992-y

ORIGINAL PAPER

Structural and functional relations between the connective tissue and epithelium of enamel organ and their role during enamel maturation

Anas F. Mahdee[1] · **Ahmed H. Ali**[1] · **James I. Gillespie**[2]

Received: 21 January 2021 / Accepted: 2 June 2021

Abstract
The morphological and possible functional interactions between the connective tissue and enamel organ cells were examined during the maturation phase of enamel formation, using immunohistochemical techniques. Decalcified mandibular sections (10 µm) including incisors were used from Wistar rats ages 10–12 weeks. Sections were incubated with one or two primary antibodies targeting cell cytoskeleton (vimentin, α-actin, α-tubulin), dendritic marker (OX6), gap junctions (cx-43), enzymes (nitric-oxide synthase (nos1) and cyclooxygenase (cox1)), and the ion transporters (Na^+/H^+ exchanger (NHE1) and Na^+/Ca^{2+} exchanger (NCX)) for 24 h, before incubation with the appropriate conjugated fluorescent secondary antibodies. Sections were examined by fluorescence microscopy. Haematoxylin–eosin slides were also employed. Cellular heterogeneity and morphological modulations were identified within enamel organ cells and connective tissue covering suggesting complex cellular interactions and indicating a new functional concept and possible complementary role during enamel maturation. Also, some ion transportation activity, and nos1 and cox1 signalling pathways have been identified, indicating intercellular communication between these regions. A hypothesis is suggested, to explain the morphological modulation of ameloblasts and papillary cells during enamel maturation which functions to increase the transporting membrane surface area to accomplish faster and bulker ion transportation to achieve controlled pH and to direct Ca^{2+} towards enamel.

Keywords Enamel organ · Enamel maturation · Interstitial cells · Ameloblast · Papillary layer · Connective tissue

Introduction

Amelogenesis is a complex physiological process that occurs within the enamel organ to underpin the formation of enamel. It has been suggested that the enamel organ consist of avascular epithelial layers where the inner most stratified layer, ameloblasts, are responsible for the secretion of an initial non-collagenous protein matrix (Lacruz et al. 2017). Following this phase, secretion of large quantities of calcium and phosphate ions, and formation of unique architecture of hydroxyapatite crystals form rods and interrods (Cui and Ge 2007; Smith and Nanci 1995). The vascular supply has been described to be within the connective tissue overlying the enamel organ epithelia (El-Agroudi et al. 1998). However, the specific processes that control the transportation and secretion of organic and inorganic materials from the vascularised connective tissue region through the avascular epithelium of enamel organ toward enamel is poorly understood.

Throughout the period of enamel formation, the ameloblast (Am) cells undergo substantial structural remodelling from a short columnar form in the early differentiation stage, to tall, well developed cells with apical processes (Tomes' process) during secretory phase. At this stage, the cells are described as being in the secretory phase. This is followed by a loss of the Tomes' processes, shortening and widening of ameloblasts, to be changed into mineral releasing cells during the maturation phase (Smith and Nanci 1995). Within the latter phase, the ameloblasts undergo cyclic morphological remodelling from ruffled-ended to smooth-ended ameloblasts (Josephsen et al. 2010). The tight junctions between ameloblasts are also remodelled between the apical border in

✉ Anas F. Mahdee
a.f.mahde@codental.uobaghdad.edu.iq

[1] Department of Restorative and Aesthetic Dentistry, College of Dentistry, University of Baghdad, Baghdad, Iraq

[2] Department of Urology, Campus Drie Eiken, University of Antwerp, Antwerp, Belgium

Published online: 07 June 2021

the ruffle-ended to the opposite basal border in the smooth-ended ameloblasts (Josephsen and Fejerskov 1977). This is associated with cyclic changes in the pH of the enamel surface from acidic (pH 6) during ruffled-ended ameloblasts to neutral (pH 7) during the smooth ameloblasts (Sasaki et al. 1991). However, the control for these cellular remodelling process and cyclic ions secretion has not yet been identified.

The outer epithelial layers of the enamel organ also undergoes changes as the enamel organ develops. In the initial secretory phase, the epithelium consists of different layers; stratum intermedium, stellate reticulum. In the maturation phase the outer epithelium cells are enlarged and changed to be more morphologically homogeneous as papillary cells. These cells are rich in mitochondria and form series of highly folded tightly packed ridges (Kallenbach 1967). Between these ridges blood vessels are seen to descend from the connective tissue layer forming complex vascular beds (El-Agroudi et al. 1998). An addition cell type, described as dendritic cells, have also been detected within the papillary folds, but their functional role within this organ is still unknown (Nishikawa and Sasaki 1999, 2000).

Because there appears to be a distinct spatial relation between the enamel organ epithelium and the covering connective tissue, this study employed immunofluorescent techniques to identify the components of possible functional interactions between these tissues by using especially selected antibodies related to cellular cytoskeleton, signalling, and ion transportation processes.

Materials and methods

Twenty male Wistar rats, 10–12 weeks of age (350–400 g) were used in this study to obtain about 40 mandibular incisor samples in this study. Animals were killed in CO_2 chamber, according to schedule 1 UK Home Office guidelines. The mandibles were dissected and divided into two halves. Each half mandible, which included the mandibular incisor, was fixed by immersion in 5 ml of 4% paraformaldehyde in phosphate buffer saline for 24 h at 4 °C. Then, specimens were washed thoroughly with distilled water before demineralisation in 17% EDTA for 2–4 weeks at 37 °C with continuous agitation using shaking incubator (Environ-shaker, Lab-line, Jencons Scientific Ltd) (Mahdee et al. 2016). The demineralised specimens were washed thoroughly with distilled water and incubated in graded sucrose solutions (10%, 20%, and 30%) for 24 h each at 4 °C for cryoprotection. Samples were then snap frozen in liquid nitrogen and stored in a − 80 °C freezer. Each frozen sample was aligned on its sagittal plane to be sectioned parallel to its long axis by using cryotome (Shandon Cryotome FSE, Thermo Fisher scientific, USA), which made it possible to visualize the rat incisor in a single section and locate the maturation phase of the ameloblasts. Sections were collected after reaching the centre of the sagittal plane where 10–15 sections (10 µm thickness) were obtained from each sample. These sections were then rapped and stored at − 80 °C. Two slides from each specimen were further fixed by immersion into 40% formal calcium for 1 h before staining with haematoxylin and eosin stain. Other slides were processed by immunohistochemistry staining according to the procedure described in Mahdee et al. (2016). In brief, the method of staining included single or double labelling with antibodies targeting cell structure or functional proteins (details for those antibodies illustrated in Table 1). Slides were incubated with primary antibodies for 24 h at 4 °C before washing and staining with the appropriate conjugated secondary fluorescence antibody (1 h at room temperature), before washing and embedding in Vectashield hard set mounting medium with dapi (Vector Laboratories Inc, Burlingame, USA). Negative control slides were prepared: (i) by using the appropriate blocking peptide, specific for the antibodies used and employing isotope controls. These negative controls staining including Human alpha smooth muscle actin blocking peptide (Abcam cat# ab 211918, UK) designed specifically for the α-actin used in this study. Additionally, rabbit IgG monoclonal (EPR25A) isotype control (1:500 Abcam cat# ab172730, UK) and normal mouse IgG1 (1:500 Santa Cruz Biotechnology cat# sc-3877 UK) were also employed. (ii) by using the secondary fluorescent antibodies without the tissue specific primary markers (Mahdee et al. 2018).

Eighty slides were examined for each stain to validate the staining patterns for each antibody and to confirm consistency and accuracy of the staining procedure. Slides were examined on an Olympus BX61 microscope (Olympus Corporation, Tokyo Japan) and images were captured with a microscope-mounted Olympus XM10 monochrome camera. Images were processed and analysed using ImageJ software (Java-based image processing program-National Institute of Health (USA)).

Results

All of the sections used in this study were taken from demineralised sagittal sections of the rat mandibular incisors exploring the maturation stage of enamel formation within the enamel organ. Figure 1 illustrates the major components and cell types within the enamel organ at this stage. The ameloblasts (Am) appear as a layer of columnar cells devoid of apical processes (Tomes' processes). The adjacent epithelial layer, the papillary layer (PL), lying above the ameloblasts is highly folded forming ridges within the organ. Above the papillary layer is a region of connective tissue (CT) within which there is a dense infiltration of blood vessels (arterioles and venules). Capillaries containing red

Table 1 Primary antibody markers used in this study

Abb	Antibody (conc.) (purpose for use)	Supplier
vim	Mouse monoclonal anti-vimentin (1:5000) (cell structural antibody to detect intermediate filaments)	BioGenex, Launch Diagnostics cat# MU074-UC, UK
α-actin	Rabbit monoclonal anti-α smooth muscle actin (1:200) (cell structural antibody to detect microfilaments)	Abcam cat# ab32575, UK
α-tub	Rabbit polyclonal anti-α tubulin (1:1000) (cell structural antibody to detect microtubules)	GeneTex, cat# GTX102078, USA
OX6	Mouse monoclonal anti-MHC class II (RT1-B) (1:200) (structural marker for mature dendritic cells)	GeneTex, cat# GTX76190, USA
cx-43	Goat polyclonal anti-connexin 43 (1:500) (gap junctions marker)	Santa Cruz Biotech cat# sc-6560, UK
nos1	Rabbit polyclonal anti-neuronal nitric oxide synthase enzyme-1 (1:500) (functional marker, cell signalling mechanism)	Santa Cruz Biotech, cat# sc-648, UK
cox1	Gout polyclonal anti-cyclooxygenase-1 (1:100) (functional marker, cell signalling mechanism)	Santa Cruz Biotech, cat# sc-1752, UK
NaK-ATPase	Rabbit monoclonal anti-sodium potassium-ATPase enzyme (1:500) (functional marker, ion transporter)	Abcam cat# Ab76020, UK
NHE1	Rabbit polyclonal anti-sodium hydrogen exchanger-1 (1:500) (functional marker, ion transporter)	Santa Cruz Biotech, cat# sc-28758, UK
NCX	Rabbit polyclonal anti-sodium calcium exchanger-1 (1:500) (functional marker, ion transporter)	Santa Cruz Biotech, cat# sc32881, UK

blood cells can be seen to lie between the folds of the papillary region that presumably arise from vessels in the connective tissue layer. The connective tissue covering the enamel organ is characterised within the current study depending on the microvasculature bed distribution. The first or deep region (* in Fig. 1a) appears as a dense connective tissue with capillaries which extend towards and integrated with the adjacent papillary layer (PL) to be closer to the ameloblasts, about one papillary cell thickness apart. The papillary layer from the other side projects toward the connective tissue in forms of long ridges. The connective tissue cells within this region are found above the papillary ridges which then extended between the capillaries and papillary ridges. These cells are termed 'interstitial cells' in the present study. The second region composed of loose connective tissue containing the arterioles, then, large flattened vessels (venules) run close to the alveolar bone. (Fig. 1b) shows the distribution of immuno-reactivity to α-smooth muscle actin (α-actin) within the enamel organ cells. Immuno-reactivity is seen within the wall of the arterioles and venules in the connective layer, within the papillary cells and strongly on the basal margins of the smooth-ended ameloblasts or the distal border in ruffle-ended ameloblasts (see Fig. 5c, d respectively). It is noteworthy that no α-actin can be detected in the blood vessels or cells lying in the connective tissue folds within the papillary cell layer.

Cells within the connective tissue layer are readily identified using the marker for intermediate filaments, vimentin (vim) (Fig. 2a). In addition, vimentin positive cells can be identified within the papillary folds and over the papillary ridges (Fig. 2b). Immuno-reactivity to a dendritic cell marker (OX6) is illustrated in (Fig. 2c), and shows the presence of dendritic cells deep within the folds of the papillary layer and also associated with the arterioles and venules of the connective tissue.

Immuno-reactivity to another cytoskeleton component, α-tubulin (α-tub), was also explored (Fig. 3). The immunolabelling of this antibody appears within the connective cells in all parts including the interstitial cells between papillary folds. Thus, the connective tissue between the papillary folds includes different cell types (vimentin and tubulin positive cells, dendritic cells) in addition to capillaries.

In order to gain some insight into possible functional interactions, the distribution of putative cell signalling and functional elements was explored (Figs. 4 and 5). Dense immuno-labelling with an antibody to nitric oxide (nos1) is apparent within ameloblasts and with lesser intensity within papillary cells. No immuno-reactivity was detected in the cells of the connective tissue or within the papillary folds. Prostaglandin signalling cells, expressing cyclooxygenase-1 (cox1), were only detected within the papillary folds (Fig. 4). These cox1 positive cells have a circular or oval shape, appear closer to or within the capillaries.

Immuno-reactivity to functional ion transporter NaK-ATPase was detected strongly within the papillary cells (Fig. 5a). In contrast, only low levels of expression were seen within the ruffled or smooth-ended ameloblasts. Similarly, the papillary cells show more intense immunolabelling with the gap junctions antibody [connexion-43 (cx43)] than the ameloblasts (Fig. 5b). The distribution of

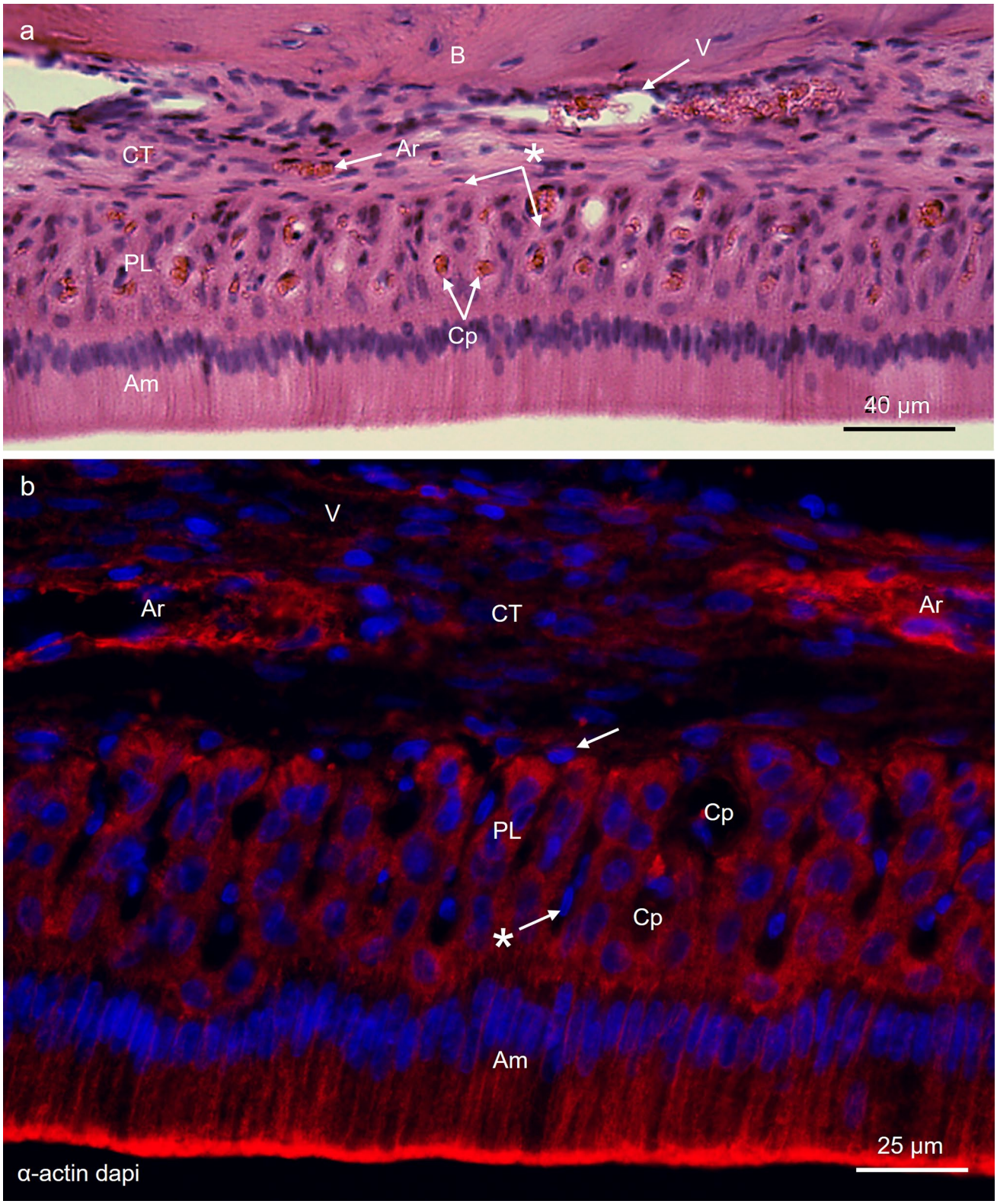

Fig. 1 Sagittal sections of the enamel organ in the maturation stage of a rat mandibular incisor stained for haematoxylin and eosin (H&E) panel (**a**) and α-smooth muscle actin (α-actin) panel (**b**). In (**a**), different structures of enamel organ can be identified: ameloblast cells (Am), papillary layer (PL), covering connective tissue (CT), capillaries (Cp) invaginated deeply between ridges of the papillary cells, arteriole (Ar), and flattened venule (V) close the alveolar bone (*). Similar section is shown in (**b**) identifying α-actin immuno-reactivity within Am and PL cells in addition to the walls of the arterioles (Ar) within connective tissue (CT). No α-actin immuno-labelling was identified within the connective tissue cells found interstitially (*) or above the papillary ridges (arrow)

cx43 immuno-reactivity appears punctuate or granular and to lie between individual papillary cells and the papillary cells and the ameloblasts. Within the later cell layer, the cx43 appear as smaller granules on the lateral membranes between ameloblasts in their different types (ruffled and smooth-ended).

Immuno-reactivity to the sodium-hydrogen exchanger (NHE-1) was detected and this appears to be different between ruffled and smooth border ameloblasts (Fig. 5e, f respectively). NHE-1 immuno-reactivity is particularly strong within the connective tissue cells between the papillary folds in both the ruffled and smooth ameloblast phases. NHE-1 staining in the ameloblasts is present but low in the ruffled ameloblasts and more strongly expressed in the smooth phase especially within the lateral cell membrane.

The expression of a further ion transporter, the sodium-calcium exchanger (NCX), was explored (Fig. 6). The expression of this antibody appeared to be similar in both smooth and ruffled ended phases at the different cellular compartment of the enamel organ. The highest immuno-reactivity to NCX is apparent within only a portion of the ameloblasts, dendritic cells and a population of cells covering the papillary ridges (Fig. 6b).

No specific tissue labelling has been observed within the negative control sections.

Discussion

All living tissues are basically composed of several types of cells which are developmentally, spatially, and physiologically integrated to perform their goals. The enamel forming cells, the ameloblasts and the outer epithelial cells of the enamel organ have been the focus of much research (Lacruz et al. 2017; Smith and Nanci 1995), although there are other cells including dendritic cells (Nishikawa and Sasaki 2000) and the covering connective cells which may have intimate spatial and functional interaction with the adjacent enamel forming cells. Additionally, the vascular source required for the viability and function of the enamel organ is located within the wrapping connective tissue which may confirm the functional integration between these different cells. Therefore, the present study employed immunohistochemistry, using of different antibodies, targeting cell cytoskeleton, cellular signalling and ion transportation that could be used to identify structural and functional interactions between enamel organ and the covering connective tissue. Since the rat mandibular incisor is a continuous growing tooth, it offers a good model in studying the whole sequences of amelogenesis (Warshawsky and Smith 1974) with a manageable size and can be easily dissected (Mahdee et al. 2018).

The intimate integration between the enamel organ epithelium and connective tissue is clearly illustrated within the current study through the spatial relationship between the capillary network and the papillary ridges. A highly organised microvasculature has been previously reported to be engaged within enamel organ, which showed an interruption at the cementoenamel junction on the mesial and distal sides of the enamel organ along the developing rat incisor (El-Agroudi et al. 1998). Therefore, the connective tissue, what was previously called periodontal tissue on the labial side of the rat incisor where the enamel is only present, is different in its structure and microvasculature to the other sides of the tooth which have no enamel (Sasaki et al. 1984). Additionally, larger arterioles have been identified in the current study lying above the papillary ridges through α-actin immuno-labelling for their muscular walls, and large sinusoid veins at the end of connective tissue region closer to the alveolar bone. This is in agreement with El-Agroudi et al. (1998), who classified the microvasculature bed covering the enamel organ into deep, intermediate and outer layers.

According to the finding of the current study the connective tissue covering enamel organ was composed of cells that were mainly immuno-labelled with vimentin and α-tubulin. While, the enamel forming cells were immunoreactive to α-actin. These markers have been identified within the odontoblast and other pulp cells (Mahdee et al. 2016). In addition, the dendritic cells were also illustrated within the papillary layer that were immunolabelled with OX6 marker (see Fig. 7a). This heterogeneity among the cells present within the enamel organ and the covering connective tissue could reflect the complexity of these tissues and the possible complementary rule during enamel maturation process. Furthermore, the morphological characteristics of the connective tissue cells showed regional differences especially through cells in close vicinity to the papillary layer. This may suggest a functional interaction between these cells and the adjacent papillary cells. Regarding this cellular complexity, few information is found in the literature in relation to connective tissue cells covering enamel organ. Their function during amelogenesis remains unknown (Krivanek et al. 2017; Reith 1959).

Another obvious physiological change noted in the current study (see Fig. 7b) are the long papillary ridges with several capillaries incorporation along the inter-papillary region. These ridges can be estimated to be 2–4 the size of stellate reticulum layer projections during the secretory stage (El-Agroudi et al. 1998). This implies that the surface area of the transporting membrane between epithelium and connective tissue has been totally 2–4 times larger during maturation stage. Additionally larger number of capillaries were shown to be incorporated within the papillary ridges with deeper invagination between them to be closer to ameloblast cells. These capillaries were reported to have very thin walls with numerous fenestrations facing the enamel (Sasaki et al. 1984). All these may help to increase the rate and extent of

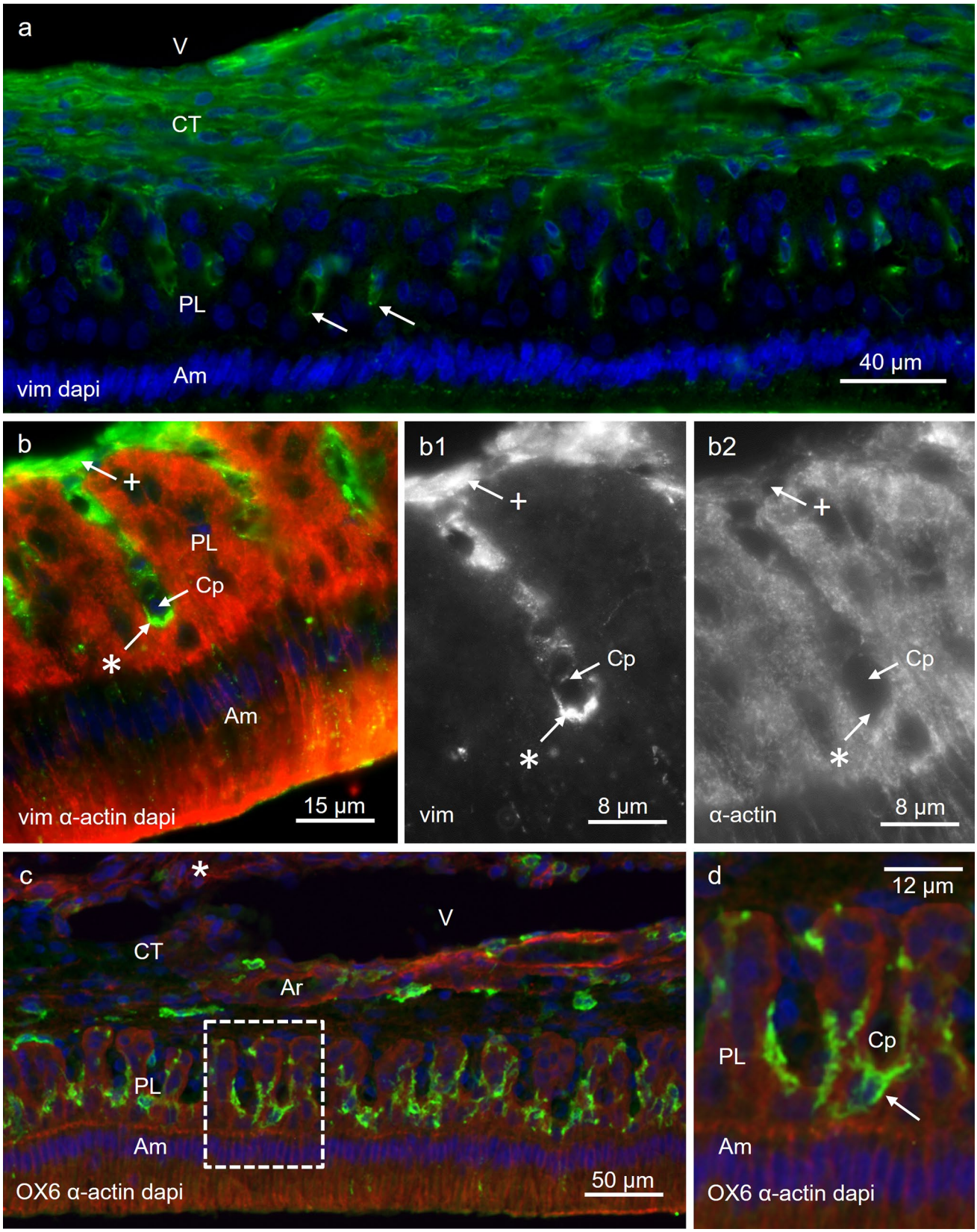

◂**Fig. 2** Demineralized sagital section of a rat mandibular incisor stained for different immunohistochemistry structural antibodies. (**a**) Stained for vimintin (vim) in green and nuclei stain (dapi) in blue. This image shows vim immuno-reactivity within connective tissue (CT) cells and the intersitial cells between paillary ridges. No vim immuno-reactivity is found in the ameloblast (Am) or the papillary cells (PL). (**b**) is composite image stained for vim in green, α-actin in red and nuclei stain (dapi) in blue to show vim immuno-reactivity (*) within interstitial connective tissue cells surrounding capillaries (Cp), and above the papillary ridges (+). Similar details are also clear in the component images (**c1**) and (**c2**) which stained for vim and α-actin respectively. Panel (**c**) stained for dendritic cell marker (OX6) in green, α-actin in red and nuclei stain dapi in blue. This section shows heavily distribution of dendritic cells (*) within papillary layer (PL) surrounding the capillaries invagination, in addition to scattered OX-6 immuno-labelling cells between papillary ridges and arterioles. The region of interest in (**c**) (dotted box) is illustrated at higher magnification in (**d**) to show the position of the dendritic cell (arrow) within the papillary layer surrounding a capillary (Cp). (Color figure online)

ion transportation from capillaries towards the mineralising enamel.

Another important observation in this study is the spatial relationship between the dendritic cells and the capillaries. Most of these cells were observed in close vicinity to the capillaries and sending their cellular processes toward them. There are studies reporting the presence of dendritic cells within the enamel organ but their function was not studied (Nishikawa and Sasaki 2000). However, a possible role in the engulfment process of the eliminated ameloginin enamel matrix material has been put forward (Nishikawa and Sasaki 1999) and in addition an immunological function as antigen presenting cells (Nishikawa and Sasaki 2000). Moreover, these cells have been labelled with NCX (Fig. 7c) within the current study. This possibly reflect a signalling process within these cells directing their response into different stimulus (Shumilina et al. 2011). However, further studies are required to identify such stimulus.

The current study has also identified a cyclical change in the expression of α-actin antibody between the distal borders of the ruffle-ended ameloblasts to the basal membrane of the smooth-ended ameloblasts (see Fig. 7b). This may be in agreement the cyclic modulation of ameloblast cells where the position of the tight junctional epithelium change from the apical border during ruffle-ended ameloblasts to the basal membrane during the smooth-ended ameloblasts (Bronckers 2017). This could offer more surface area of the ion exchanging membrane during the smooth-ended ameloblasts allowing all lateral and apical cellular membranes to achieve active ion transporting process. The NHE immunoreactivity also showed similar cyclic expression within different ameloblast phases that may cope with the suggested phenomena. The increase surface area within smooth ameloblast phase could add more capacity to the pH controlling process within enamel to change it from 6.2 during ruffled to 7.2 during smooth ameloblasts phases (Bronckers 2017; Josephsen et al. 2010). In addition, the apparent expression of NaK-ATPase within the papillary cells could be one of the major cellular function to produce this role through making electrochemical Na^+ gradient to maintain negative cell potential of the ameloblasts during their different modulation stages (Josephsen et al. 2010; Lacruz et al. 2013). This could be supported by cytosol coupling through the presence of gap junctions between papillary cells and ameloblasts (Al-Ansari et al. 2018). All these may support unidirectional ion pumping toward enamel.

The isoform of nitric oxide synthase examined in this study was the neuronal type, nNOS (nos1). Nitric oxide is a neurotransmitter and signalling molecules which has central and peripheral function. Centrally, it involves in memory, learning and controlling of blood pressure, whilst peripherally it helps to reduce vascular tone causing vasodilation by its effect on the smooth muscles (Förstermann and Sessa 2012). The presence of nos1 has been previously demonstrated within ameloblasts during all stages of enamel formation and with less intensity within papillary layer during enamel maturation (Mahdee et al. 2017). This could indicate the role of ameloblasts and the papillary cells in controlling vascular tone within the covering connective tissue. Also the presence of nos within cells achieving continuous morphological and functional modulations could suggest the role of this neurotransmitter within this process through autocrine or paracrine signalling pathways. On the other hand, cox1 immunoreactivity has been identified within some interstitial cells between and covering papillary ridges. The relation between nitric oxide and prostaglandin signalling pathways has been identified within different organs (Sorokin 2016) including the pulp (Alhelal 2016). This may indicate cellular cross talking between the epithelium and connective tissue of the enamel organ, however the purpose for such cellular interactions need further investigations.

Although the role of the enamel epithelium in transporting systematic Ca^{2+} to enamel has been identified, the mechanisms behind this ion transportation is far from clear (Nurbaeva et al. 2017). The dominant paradigm for Ca^{2+} transportation has been agreed to be transcellular route (Bawden 1989; Nurbaeva et al. 2017), especially through studies showing the lack for diffusion of horseradish peroxidase and lanthanum across intercellualr junctions between ameloblasts (Takano 1995; Takano and Crenshaw 1980). According to the results of the present study, high intensity of NCX1 immunolabelling was identified within the ameloblasts during maturation stage. This is in agreement with Okumura et al. (2010) who first reported the present of NCX1 and NCX3 within the mature ameloblasts. However, they claimed the localization of this ion transporter on the apical membrane, whilst the current study has shown in clear and highly magnified images that NCX1 was active within the whole ameloblast cell including apical, middle

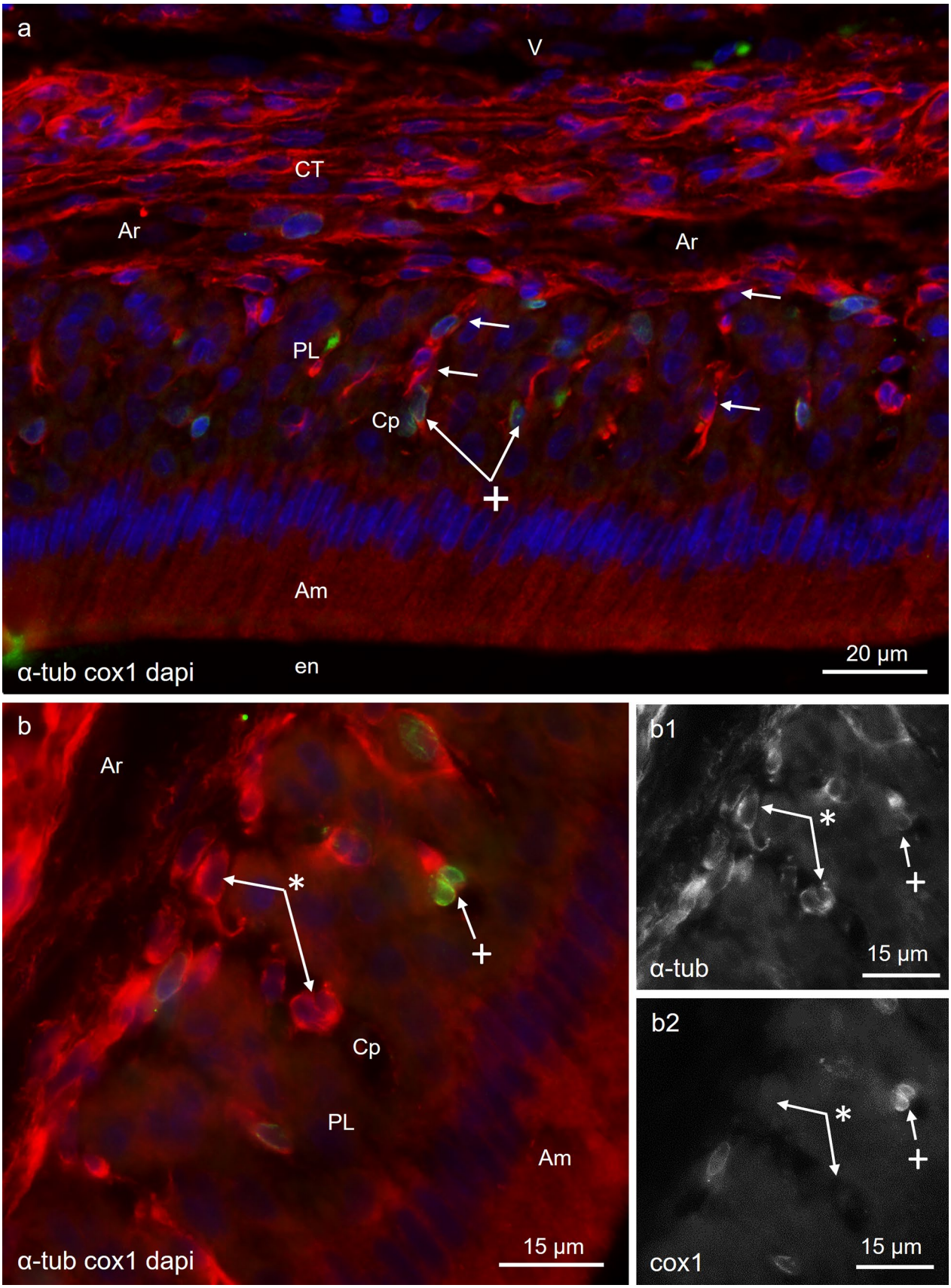

◂**Fig. 3** Sagittal sections of the rat mandibular incisor showing the enamel organ connective tissue in the maturation stage. (**a**) and, (**b**) were stained for α-tubulin (α-tub) in red, cyclooxygenase-1 (cox1) in green and dapi in blue, while (**b1**) and (**b2**) are component images for (**b**) stained for α-tub and cox respectively. (**a**) is an overview image showing the deep capillaries (Cp) laying among the papillary layer (PL) ridges, arterioles (Ar) within the intermediate connective tissue (CT), and the venules (V) within the outer connective tissue. There are cells (arrows) descending from the inner CT interstitially between capillaries and papillary ridges. Some of these cells showing cox immuno-reactivity. Similar observations but with higher magnification are illustrated in (**b**) and its component images (**b1**) and (**b2**). These panels show the interstitial cells located near capillaries (Cp), and are immune-labelled to both cox-1 (+) and α-tub or to α-tub (*) only. (Color figure online)

and basal regions. Regarding the function of NCX, it is a bidirectional electronic transporter exchanging one Ca^{2+} for three Na^{+} ions. Therefore, it depends on the membrane concentration potentials for Na^{+} and Ca^{2+} ions to accomplish influx or efflux of Ca^{2+} (Nurbaeva et al. 2017). As mentioned previously, due to the intensive activity of NaK-ATPase within the papillary cells, this increases the Na^{+} concentration within the extracellular fluid between cells (see Fig. 7c). This may activate the NCX on the basal part of the ameloblasts to intrude Ca^{2+} inside the ameloblasts. There are several reported scenarios to buffer the intracellular Ca^{2+} [Ca^{2+}]i within ameloblasts (Bronckers 2017; Nurbaeva et al. 2017). These may include calcium binding proteins (parvalbumin, calbindin, calretinin, calmodulin etc.) which are able to bind and transport Ca^{2+} from basal to apical direction without raising [Ca^{2+}]i (Davideau et al. 1993; Kördel et al. 1993). Another intracellular regulating method that has been presented within ameloblasts is ATPase pumps including; sarcoplasmic reticulum Ca^{2+}-ATPase (SERCA) to pump cytosolic [Ca^{2+}]i into the endoplasmic reticulum, and plasma membrane Ca^{2+}-ATPase (PMCA)] as active Ca^{2+} pumping procedures toward enamel (Franklin et al. 2001; Zaki et al. 1996). Also passive ion exchangers [NCX and K^{+} dependant Na^{+}/Ca^{2+} exchanger (NCKX)] are also present, which passively efflux Ca^{2+} toward enamel (Hu et al. 2012; Okumura et al. 2010). This also supports the presence of NCX immunoreactivity within the apical region of ameloblasts in the current study as an efflux route for Ca^{2+} toward enamel.

It should be noted that intense immunoreactivity to NCX was seen within the interstitial cells of the connective tissue. These cells were identified in close vicinity to capillaries. As it has been shown that the NCX exchanger can function bi-directionally, there are two possibilities for this NCX immunoreactivity within these cells; either influx of Ca^{2+} into the cells or efflux of Ca^{2+} out of these cells. If the first possibility is considered, Ca^{2+} influx may have a broad role within cellular signalling processes (Berridge et al. 2003). These need to be identified in further studies. In addition, if the second possibility is operating, Ca^{2+} efflux will increase extracellular Ca^{2+} concentration which may facilitate Ca^{2+} diffusion to the enamel organ. All these possibilities are raising questions about the exact role of these interstitial cells during the process of amelogenesis.

In conclusions a new concept has been suggested that the process of enamel maturation is a complex series of interrelated physiological process. These are more complex than what previously suggested in the literature, involving multiple cell types including enamel organ epithelium, dendritic cells and the covering connective tissue. New ideas about the possible physiology processes behind cellular morphological changes during enamel maturation phase within the papillary layer and ameloblasts have been suggested. These cellular morphological changes could play a pivotal role in the process of ion transportation to control pH and Ca^{2+} movement during this stage of enamel formation.

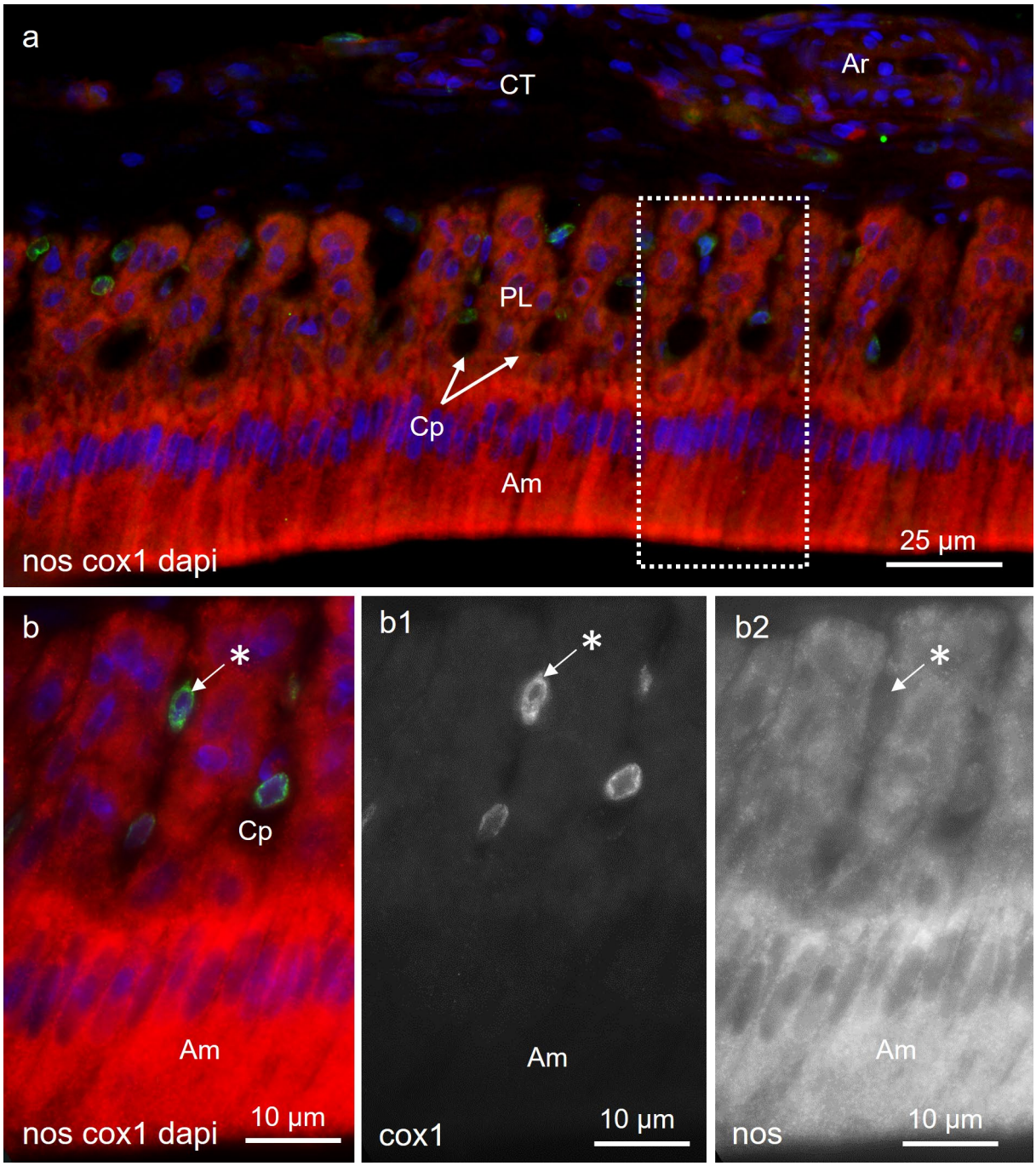

Fig. 4 Expression of nitric oxide (nos) and cyclooxygenase-1 (cox1) within sagittal sections of the rat mandibular incisor enamel organ during maturation stage. (**a**, **b**) Was stained for nos in red, cox1 in green and dapi in blue, and (**b1**, **b2**) are component images of (**b**) stained for cox1 and nos respectively. A high intensity of nos immuno-reactivity is observed within ameloblasts (Am) and less in papillary layer (PL) and the least within arterioles (Ar). A highlighted region in (**a**) is illustrated at higher magnification in (**b**) and its component images **(b1)** and **(b2)**. These images show cells (*) within the interstitial CT close to capillaries (Cp) are immuno-labelled to cox, while other papillary layer cells and ameloblasts are immuno-reactive to nos. (Color figure online)

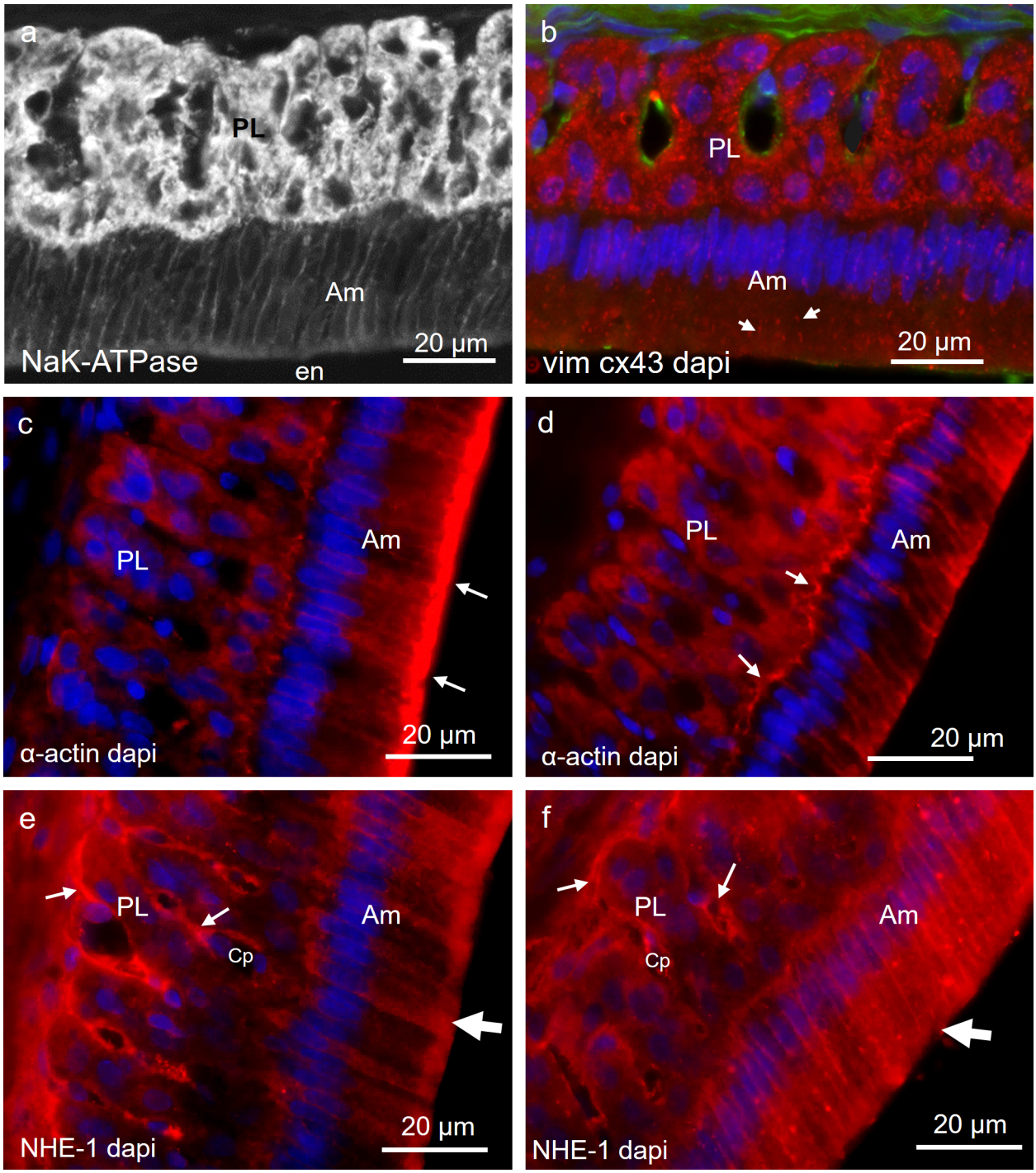

Fig. 5 Sagittal sections of the enamel organ of the rat mandibular incisor stained for different antibodies during the maturation stage. (**a**) Stained for NaK-ATPase presented with high expression within papillary layer. The composite image (**b**) stained for vimentin (vim) in green, connexion-43 (cx43) in red and dapi in blue. The immunolocalization of cx43 appears as punctuated or granular which are highly expressed within the papillary layer and less so on the lateral walls between ameloblasts (arrows). The changes in ameloblast cells between ruffled and smooth border are represented in images (**c**, **e**) and (**d**, **f**) respectively. Images (**c**) and (**d**) were stained for α-actin (red) and dapi (blue). The differences in immunoreactivity of α-actin is apparent in the distal membrane (arrows) of the ruffle-ended ameloblasts in **(c)**, while in the basal membrane (arrows) of smooth-ended ameloblasts in (**d**). Images (**e**, **f**) were stained for sodium-hydrogen exchanger (NHE-1: red) and dapi (blue). Both images show immuno-labelling of NHE-1 within interstitial cells of CT near capillaries (Cp) and above papillary layer (PL) (arrows), in the distal border of ruffled ameloblasts (Am) (thick arrow in image 2), and within lateral membranes of smooth-ended Am (thick arrow in **f**). (Color figure online)

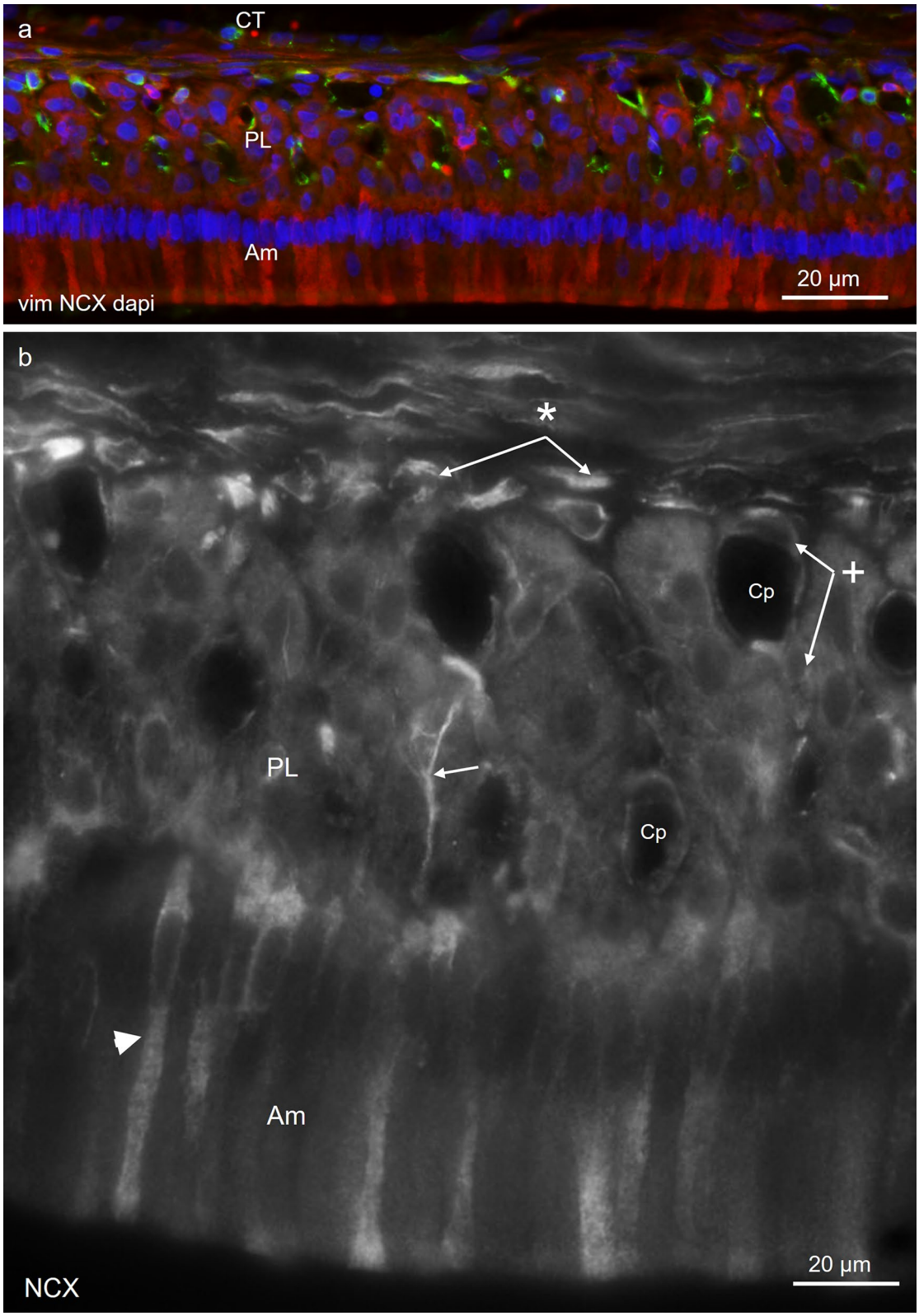

Fig. 6 Sagittal sections of the enamel organ of the rat mandibular incisor showing expression of sodium calcium exchanger (NCX) during the maturation stage. (**a**) Stained for vim (green), NCX in red and dapi (blue), while (**b**) only stained for NCX. In (**a**) the expression of NCX appears within the epithelial cells of enamel organ (Am and PL) and the connective tissue cells above PL. At higher magnification (**b**) the higher expression of NCX is illustrated within some of the ameloblasts (Am) (arrow head), dendritic cell (arrow) within PL, and the connective tissue cells (*) above PL. Less intensity of NCX staining is identified within PL cells and the interstitial cells (+) surrounding capillaries (Cp). (Color figure online)

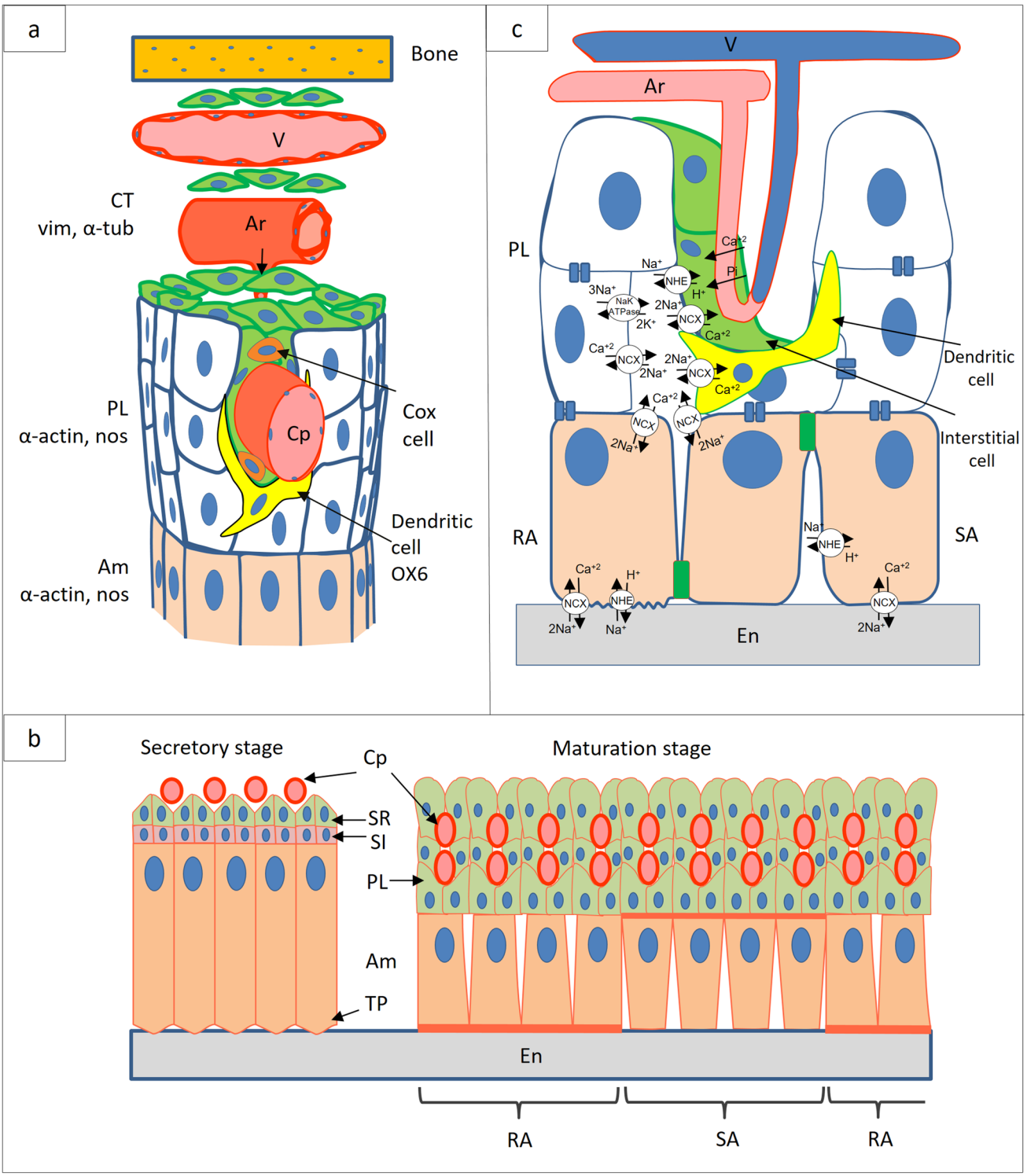

Fig. 7 Schematic representation of the enamel organ cells. (**a**) Represents a three-dimension illustration of the enamel organ and connective tissue regions with their microvasculature bed. (**b**) Shows morphological cellular changes between secretory and maturation stages of enamel organ. (**c**) Illustrates the ion transportation during maturation stage. The following structures have been shown: Ameloblasts (Am), papillary layer (PL), connective tissue cells (CT), arteriole (Ar), vein (V), capillary (Cp), enamel (En), tomes' process (TP), ruffle-ended ameloblasts (RA), smooth-ended ameloblasts (SA), stratum intermedium (SI), and stellate reticulum (SR)

Acknowledgements The authors would like to thank Dr. John M. Whitworth (Professor of Endodontology at the School of Dental Sciences/Newcastle University) for his support of this work and Mrs D.S. Jones for proofreading the final manuscript.

Author contributions All authors contributed to the study conception and design. Material preparation, data collection and analysis were performed by [Anas F. Mahdee], and [James I. Gillespie]. The first draft of the manuscript was written by [Anas F. Mahdee] and all authors commented on previous versions of the manuscript. All authors read and approved the final manuscript.

Funding No funding was received for conducting this study.

Data availability All data and materials have been listed within the manuscript.

Code availability Not applicable.

Declarations

Conflict of interest The authors have no conflicts of interest to declare that are relevant to the content of this article.

Consent to participate For this type of study, formal consent is not required.

Consent for publication For this manuscript, consent for publication is not required.

Ethical approval The animal work was performed according to the schedule 1, UK Home Office guidelines, within the facilities of the Oral Biology Department in the Institute of Cellular Medicine, Newcastle University. All applicable international, national, and/or institutional guidelines for the care and use of animals were followed.

References

Al-Ansari S, Jalali R, Plotkin LI, Bronckers AL, DenBesten P, Zhang Y, Raber-Durlacher JE, de Lange J, Rozema FR (2018) The importance of connexin 43 in enamel development and mineralization. Front Physiol 9:750

Alhelal A (2016) Physiological and molecular responses in the pulp associated with early inflammatory process. PhD thesis submitted to Newcastle University UK. https://api.semanticscholar.org/. CorpusID:90023804

Bawden JW (1989) Calcium transport during mineralization. Anat Rec 224:226–233

Berridge MJ, Bootman MD, Roderick HL (2003) Calcium signalling: dynamics, homeostasis and remodelling. Nat Rev Mol Cell Biol 4:517–529

Bronckers A (2017) Ion transport by ameloblasts during amelogenesis. J Dent Res 96:243–253

Cui FZ, Ge J (2007) New observations of the hierarchical structure of human enamel, from nanoscale to microscale. J Tissue Eng Regen Med 1:185–191

Davideau J, Celio M, Hotton D, Berdal A (1993) Developmental pattern and subcellular localization of parvalbumin in the rat tooth germ. Arch Oral Biol 38:707–715

El-Agroudi MA, Selliseth NJ, Selvig KA (1998) Microvascular system of the rat incisor enamel organ. A scanning electron microscopic study of vascular corrosion casts. Eur J Oral Sci 106:1013–1021

Förstermann U, Sessa WC (2012) Nitric oxide synthases: regulation and function. Eur Heart J 33:829–837

Franklin IK, Winz RA, Hubbard MJ (2001) Endoplasmic reticulum Ca2+-ATPase pump is up-regulated in calcium-transporting dental enamel cells: a non-housekeeping role for SERCA2b. Biochem J 358:217–224

Hu P, Lacruz RS, Smith CE, Smith SM, Kurtz I, Paine ML (2012) Expression of the sodium/calcium/potassium exchanger, NCKX4, in ameloblasts. Cells Tissues Organs 196:501–509

Josephsen K, Fejerskov O (1977) Ameloblast modulation in the maturation zone of the rat incisor enamel organ. A light and electron microscopic study. J Anat 124:45

Josephsen K, Takano Y, Frische S, Praetorius J, Nielsen S, Aoba T, Fejerskov O (2010) Ion transporters in secretory and cyclically modulating ameloblasts: a new hypothesis for cellular control of preeruptive enamel maturation. Am J Physiol Cell Physiol 299:C1299–C1307

Kallenbach E (1967) Cell architecture in the papillary layer of rat incisor enamel organ at the stage of enamel maturation. Anat Rec 157:683–697

Kördel J, Skelton NJ, Akke M, Chazin WJ (1993) High-resolution solution structure of calcium-loaded calbindin D9k. J Mol Biol 231:711–734

Krivanek J, Adameyko I, Fried K (2017) Heterogeneity and developmental connections between cell types inhabiting teeth. Front Physiol 8:376

Lacruz RS, Habelitz S, Wright JT, Paine ML (2017) Dental enamel formation and implications for oral health and disease. Physiol Rev 97:939–993

Lacruz RS, Smith CE, Kurtz I, Hubbard MJ, Paine ML (2013) New paradigms on the transport functions of maturation-stage ameloblasts. J Dent Res 92:122–129

Mahdee A, Alhelal A, Eastham J, Whitworth J, Gillespie J (2016) Complex cellular responses to tooth wear in rodent molar. Arch Oral Biol 61:106–114

Mahdee A, Eastham J, Whitworth J, Gillespie J (2018) Evidence for programmed odontoblast process retraction after dentine exposure in the rat incisor. Arch Oral Biol 85:130–141

Mahdee AF, Alhelal AG, Whitworth J, Eastham J, Gillespie J (2017) Evidence for complex physiological processes in the enamel organ of the rodent mandibular incisor throughout amelogenesis. Med J Babylon 14:68–82

Nishikawa S, Sasaki F (1999) Internalization of amelogenin by dendritic cells of the papillary layer during transition and early maturation stages. Histochem Cell Biol 112:301–305

Nishikawa S, Sasaki F (2000) Detection of immature dendritic cells in the enamel organ of rat incisors by using anti-cystatin C and anti-MHC class II immunocytochemistry. J Histochem Cytochem 48:1243–1255

Nurbaeva MK, Eckstein M, Feske S, Lacruz RS (2017) Ca2+ transport and signalling in enamel cells. J Physiol 595:3015–3039

Okumura R, Shibukawa Y, Muramatsu T, Hashimoto S, Nakagawa K-I, Tazaki M, Shimono M (2010) Sodium-calcium exchangers in rat ameloblasts. J Pharmacol Sci 112:223–230

Reith EJ (1959) The enamel organ of the rat's incisor, its histology and pigment. Anat Rec 133:75–89

Sasaki S, Takagi T, Suzuki M (1991) Cyclical changes in pH in bovine developing enamel as sequential bands. Arch Oral Biol 36:227–231

Sasaki T, Tominaga H, Higashi S (1984) Microvascular architecture of the enamel organ in the rat-incisor maturation zone. Scanning and transmission electron microscopic studies. Cells Tissues Organs 118:205–213

Shumilina E, Huber SM, Lang F (2011) Ca2+ signaling in the regulation of dendritic cell functions. Am J Physiol Cell Physiol 300:C1205–C1214

Smith CE, Nanci A (1995) Overview of morphological changes in enamel organ cells associated with major events in amelogenesis. Int J Dev Biol 39:153–161

Sorokin A (2016) Nitric oxide synthase and cyclooxygenase pathways: a complex interplay in cellular signaling. Curr Med Chem 23:2559–2578

Takano Y (1995) Enamel mineralization and the role of ameloblasts in calcium transport. Connect Tissue Res 33:127–137

Takano Y, Crenshaw M (1980) The penetration of intravascularly perfused lanthanum into the ameloblast layer of developing rat molar teeth. Arch Oral Biol 25:505–511

Warshawsky H, Smith C (1974) Morphological classification of rat incisor ameloblasts. Anat Rec 179:423–445

Zaki A, Hand A, Mednieks M, Eisenmann D, Borke J (1996) Quantitative immunocytochemistry of Ca2+-Mg2+ ATPase in ameloblasts associated with enamel secretion and maturation in the rat incisor. Adv Dent Res 10:245–251

Terms and Conditions

Springer Nature journal content, brought to you courtesy of Springer Nature Customer Service Center GmbH (“Springer Nature”).
Springer Nature supports a reasonable amount of sharing of research papers by authors, subscribers and authorised users (“Users”), for small-scale personal, non-commercial use provided that all copyright, trade and service marks and other proprietary notices are maintained. By accessing, sharing, receiving or otherwise using the Springer Nature journal content you agree to these terms of use (“Terms”). For these purposes, Springer Nature considers academic use (by researchers and students) to be non-commercial.
These Terms are supplementary and will apply in addition to any applicable website terms and conditions, a relevant site licence or a personal subscription. These Terms will prevail over any conflict or ambiguity with regards to the relevant terms, a site licence or a personal subscription (to the extent of the conflict or ambiguity only). For Creative Commons-licensed articles, the terms of the Creative Commons license used will apply.
We collect and use personal data to provide access to the Springer Nature journal content. We may also use these personal data internally within ResearchGate and Springer Nature and as agreed share it, in an anonymised way, for purposes of tracking, analysis and reporting. We will not otherwise disclose your personal data outside the ResearchGate or the Springer Nature group of companies unless we have your permission as detailed in the Privacy Policy.
While Users may use the Springer Nature journal content for small scale, personal non-commercial use, it is important to note that Users may not:

1. use such content for the purpose of providing other users with access on a regular or large scale basis or as a means to circumvent access control;
2. use such content where to do so would be considered a criminal or statutory offence in any jurisdiction, or gives rise to civil liability, or is otherwise unlawful;
3. falsely or misleadingly imply or suggest endorsement, approval , sponsorship, or association unless explicitly agreed to by Springer Nature in writing;
4. use bots or other automated methods to access the content or redirect messages
5. override any security feature or exclusionary protocol; or
6. share the content in order to create substitute for Springer Nature products or services or a systematic database of Springer Nature journal content.

In line with the restriction against commercial use, Springer Nature does not permit the creation of a product or service that creates revenue, royalties, rent or income from our content or its inclusion as part of a paid for service or for other commercial gain. Springer Nature journal content cannot be used for inter-library loans and librarians may not upload Springer Nature journal content on a large scale into their, or any other, institutional repository.
These terms of use are reviewed regularly and may be amended at any time. Springer Nature is not obligated to publish any information or content on this website and may remove it or features or functionality at our sole discretion, at any time with or without notice. Springer Nature may revoke this licence to you at any time and remove access to any copies of the Springer Nature journal content which have been saved.
To the fullest extent permitted by law, Springer Nature makes no warranties, representations or guarantees to Users, either express or implied with respect to the Springer nature journal content and all parties disclaim and waive any implied warranties or warranties imposed by law, including merchantability or fitness for any particular purpose.
Please note that these rights do not automatically extend to content, data or other material published by Springer Nature that may be licensed from third parties.
If you would like to use or distribute our Springer Nature journal content to a wider audience or on a regular basis or in any other manner not expressly permitted by these Terms, please contact Springer Nature at

onlineservice@springernature.com